Mathematica Aeterna, Vol. 1, 2011, no. 04, 245 - 261

Effects of Thermal Radiation on Transient MHD Free Convection Flow over a vertical Surface embedded in a Porous Medium with Periodic Boundary Temperature

Promise MEBINE
Department of Mathematics/Computer Science,
Niger Delta University, Wilberforce Island, NIGERIA
Emails: p.mebine@yahoo.com, pw.mebine@ndu.edu.ng
Telephone (Mobile): +234(0) 805 3329 308

Emmanuel Munakurogha ADIGIO
Department of Mechanical Engineering,
Niger Delta University, Wilberforce Island, NIGERIA

Abstract

This paper investigates the effects of thermal radiation on transient MHD free convection flow over a vertical surface embedded in a porous medium with periodic temperature. Analytical solutions are obtained for the governing coupled dimensionless partial differential equations of velocity and temperature. The results are discussed with the effects of various dimensionless parameters such as R, radiation; M, magnetic; χ, porosity and $\Omega\tau$, phase angle for the Prandtl number, $Pr = 0.71$ which represents air at $20^o C$ and of 1 atmospheric pressure. The results showed sensitive dependence on the parameters. Also, quantitative discussions are presented for the Skin friction and Heat flux.

Mathematics Subject Classification: 76W05, 76E06, 76R10

Keywords: MHD free convection flow; periodic temperature; thermal radiation

1 Introduction

Natural or free convection flows which are caused by buoyancy or reduced gravity [24, 20] are due to spatial temperature variations that give rise to corresponding variations in the density of fluids (both gases and liquids). It is known that buoyancy induced flow within fluid-saturated porous media is

encountered in a wide range of thermal engineering applications such as in geothermal systems, oil extraction, ground water pollution, thermal insulation, heat exchangers, storage of nuclear wastes, packed bed catalytic reactors, atmospheric and oceanic circulation. Comprehensive discussions and or reviews are found in literature [13, 6, 7, 21].

The study of flow for an electrically conducting fluid has many applications in engineering problems such as magnetohydrodynamics (MHD) generators, plasma studies, nuclear reactors, geothermal energy extraction, and the boundary layer control in the field of aerodynamics [4]. Recent advances and applications of MHD based microfluidic devices are extensively reviewed in the paper by Qian and Bau [23]. Some of these devices include MHD-based micro-pumps used for producing a mechanical force which sets the fluid into motion; MHD-based microfluidic networks used for transporting fluids and reagents across networks of conduits, where the flow control typically requires the use of pumps and valves; MHD-based stirrers used for altering the flow direction to enhance dispersion, and takes advantage of the ease with which one can induce secondary flows; MHD-based liquid chromatography used for the separation, purification, and detection of various biochemicals. Although, some of these devices are fabricated with low temperature co-fired ceramic tapes [27] (e.g. MHD-based microfluidic networks), significant heat generation or radiative heat transfer occurs due to the induction of eddy currents in most of these engineering applications [17, 25, 26, 10]. Other examples are, high temperature phenomena or high-power radiation sources commonly encountered in solar physics-particularly in astrophysical studies [3], in combustion applications such as fires, furnaces, IC engines, in nuclear reactions such as in the sun or in nuclear explosions [13], in compressors in ships and in gas flares from petrochemical industry [1, 22]. For air, the contribution of radiation becomes significant when the wall temperature is in the range $6000 - 10,000K$. This situation is encountered for re-entry space vehicles. Korycki [16] described radiative heat transfer as an important fundamental phenomena existing in practical engineering such as those found in solar radiation in buildings, foundry engineering and solidification processes, die forging, chemical engineering, composite structures applied in industry. Another important feature that usually occurs in electronic devices over a period of continuous usage is the hotness of the surface. This means that a poor design could trap heat generated by the source of the power supply and could incapacitate the efficiency and durability of the systems. Therefore, the efficiency in the functioning of these systems is enhanced when they are subjected to external cooling devices like air conditioners, electric fans, and some others (e.g. laptop computers) inbuilt storage devices that store electrical energy for them to function for sometime even without external source of power supply [12]. The IC components of these electronic systems are thermally coupled to the

surrounding via convection and radiation. Radiation has a significant role in heat transfer in low-flow applications where there exists a larger temperature gradient between the components and the surrounding.

A distinguishing feature of radiative heat transfer is that it is associated with the radiation heat flux, which is proportional to the differences of individual absolute temperatures of the bodies each raised to the fourth power. This is a primary difficulty in modelling radiation heat transfer problems in that the radiation heat flux involves an integro-differential equation in the governing energy equation. Interestingly, computational fluid dynamics techniques (e.g. finite difference methods) are being used to study complex problems in fluid flow and heat transfer [8] because they are not easily amenable to analytic and algebraic techniques due to the nonlinearities involved in the governing equations. However, it is known that linear differential approximation of the radiation heat flux is available [8, 9] and is widely applied [15, 18, 19] in proffering analytical solutions. Such exact results serve as toolkits for numerical experimentations. Therefore, the use of such linear approximation can surmise the behaviour of solutions of the nonlinear system, at least near the equilibrium point.

Chaudhary and Jain [5] presented an analytical study of magnetohydrodynamic transient convection flow past a vertical surface embedded in a porous medium with an oscillating temperature. Examples abound in literature, where many industrial and technological systems are subjected to periodic heating and cooling, such as during the combustion cycle, the valves of an internal combustion engine experience direct heating from the combusting gases, cooling from the intake air and periods of thermal contact with the valve seat [14], and many other examples like heat conduction in sliding solids, regenerative heat exchangers, solar heating systems and heat conduction between the workpiece and the die in repetitive forming and rolling processes [11]. Most of such applications involve conditions of high temperature phenomena or high-power radiation sources. It is the objective of this paper, therefore, to advance analytical solutions to the problem of the effects of thermal radiation on transient MHD free convection flow over a vertical surface embedded in a porous medium with periodic boundary temperature. The analytical solutions give a wider applicability in understanding the basic physics of any problem, which are particularly important in industrial and technological fields.

In section 2, the mathematical formulation of the problem and dimensionless forms of the governing equations are established. Solution method to these equations for the flow variables are briefly examined in section 3. The results of the previous sections are discussed in section 4. In section 5, general concluding remarks of the results of the previous sections are given.

2 Mathematical Formulation

Following the arguments presented by Chaudhary and Jain [5], an unsteady free convection flow of an incompressible and electrically conducting viscous fluid along an infinite vertical plate that is embedded in a porous medium is considered. The x-axis is taken on the infinite plate and parallel to the free stream velocity and y-axis normal to it. Initially, the plate and the fluid are at the same temperature T_∞. At time $t > 0$, the plate temperature is raised to T_w and a periodic temperature is assumed to be superimposed on this mean constant temperature of the plate. A magnetic field of uniform strength B_0 is applied in the transverse direction of the plate and the induced magnetic field is neglected. The flow is in the direction of the plate such that maximum mean velocity U_m is only attainable in between the wall of the plate and far away from the plate. This implies that the flow is zero respectively at the wall of the plate and far away from the plate (see the physical model Figure 1). With the aid of the Boussinesq approximation, the governing equations of the flow for an optically thin medium are then reduced to the following system of equations:

$$\frac{\partial u}{\partial t} = \nu\frac{\partial^2 u}{\partial y^2} + g\beta\Big(T - T_\infty\Big) - \frac{\sigma_c B_0^2}{\rho}u - \frac{\nu}{k}u, \tag{1a}$$

$$\frac{\partial T}{\partial t} = \alpha_d\frac{\partial^2 T}{\partial y^2} - \frac{1}{\rho c_p}\frac{\partial q}{\partial y}, \tag{1b}$$

$$\frac{\partial q}{\partial y} = 4\,\sigma\,\alpha\left(T^4 - T_\infty^4\right), \tag{1c}$$

where $u, t, y, \rho, \alpha_d, B_0, k, \nu, \sigma_c, \alpha$ and σ represents flow, time, transverse coordinate, fluid density, thermal diffusivity, applied magnetic field strength, permeability of porous medium, kinematic viscosity, electric conductivity of the fluid, absorption coefficient or penetration depth and the Stefan-Boltzmann constant. g is the acceleration due to gravity.

The initial and boundary conditions associated to equations (1) are

$$u = 0, T = T_\infty \quad \text{for all} \quad y\,, t \le 0, \tag{2a}$$

$$u = 0\,, T = T_w + \xi(T_w - T_\infty)\cos\omega\, t \quad \text{at} \quad y = 0\,, t > 0, \tag{2b}$$

$$u \to 0\,, T \to T_\infty \quad \text{as} \quad y \to \infty\,, t > 0. \tag{2c}$$

Here ξ represents amplitude and ω, frequency of oscillation.

The radiative flux equation (1c) is highly nonlinear in T. However, when it is assumed that the temperature differences within the flow are sufficiently small, then the linear differential approximation of Cogley-Vincenti-Gilles equilibrium model [9] of the radiation flux becomes significant. In this case T^4 can

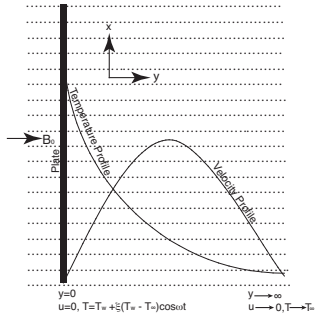

Figure 1: Physical Model.

be expressed as a linear function of temperature in Taylor series about T_∞ neglecting higher order terms. Thus,

$$T^4 \cong 4T_\infty^3 T - 3T_\infty^4. \tag{3}$$

Therefore, equation (1c) is now written as

$$\frac{\partial q}{\partial y} = 16\,\alpha\,\sigma\,T_\infty^3\Big(T - T_\infty\Big). \tag{4}$$

In order to facilitate the analysis, the following dimensionless variables and parameters are employed:

$$Y = \frac{yU_m}{\nu}\,,\quad U = \frac{u}{U_m}\,,\quad \tau = \frac{tU_m^2}{\nu}\,,\quad \Theta = \frac{T}{T_\infty}\,,\quad \Theta_w = \frac{T_w}{T_\infty}\,,\quad \Omega = \frac{\omega\nu}{U_m^2}\,,$$
$$M = \frac{\nu\sigma_c B_0^2}{\rho U_m^2}\,,\quad Gr = \frac{\nu\beta g T_\infty}{U_m^2}\,,\quad \chi = \frac{kU_m^2}{\nu}\,,\quad Pr = \frac{\nu}{\alpha_d}\,,\quad R = \frac{4\nu\alpha\sigma T_\infty^3}{\rho c_p U_m^2}. \tag{5}$$

Therefore, the dimensionless governing equations are

$$\frac{\partial^2 U}{\partial Y^2} - \frac{\partial U}{\partial \tau} + Gr\,(\Theta - 1) - (M + \frac{1}{\chi})U = 0, \tag{6a}$$

$$\frac{1}{Pr}\frac{\partial^2 \Theta}{\partial Y^2} - \frac{\partial \Theta}{\partial \tau} - R\,(\Theta - 1) = 0, \tag{6b}$$

with the initial and boundary conditions

$$U = 0\,, \Theta = 1 \quad \text{for all} \quad Y\,, \tau \leq 0, \tag{7a}$$

$$U = 0\,, \Theta = \Theta_w + \xi(\Theta_w - 1)\cos\Omega\tau \quad \text{at} \quad Y = 0\,, \tau > 0, \tag{7b}$$

$$U \to 0\,, \Theta \to 1 \quad \text{as} \quad Y \to \infty\,, \tau > 0. \tag{7c}$$

The parameters entering the problem are M, magnetic parameter; Gr, Grashof number; χ, porosity parameter; Pr, Prandtl number; Ω, frequency of oscillation, and R, radiation parameter. The mathematical statement of the problem embodies the solution of equations (6) subject to equations (7).

3 Main Analytical Results

The problem posed (6) represents a system of coupled and linear partial differential equations (PDEs). Exact results of equations (6) subject to equations (7) are herein deduced by using Laplace Transform technique [2]. The energy equation (6b) is uncoupled from the momentum equation (6a). One can advance solution for the temperature variable $\Theta(Y, \tau)$ whereupon the solution of $U(Y, \tau)$ is then derived. Therefore, the solution for the velocity and tempera-

ture are respectively given as follows:

$$
\begin{aligned}
U(Y,\tau) = \frac{a_1}{2a_4}\Bigg[& \exp\Big(\sqrt{M+\frac{1}{\chi}}Y\Big)\operatorname{erfc}\Big(\frac{Y}{2\sqrt{\tau}}+\sqrt{\tau(M+\frac{1}{\chi})}\Big) \\
& +\exp\Big(-\sqrt{M+\frac{1}{\chi}}Y\Big)\operatorname{erfc}\Big(\frac{Y}{2\sqrt{\tau}}-\sqrt{\tau(M+\frac{1}{\chi})}\Big)\Bigg] \\
-\frac{a_1}{2a_4}\exp\Big(-\frac{a_4}{a_3}\tau\Big)\Bigg[& \exp\Big(\sqrt{M+\frac{1}{\chi}-\frac{a_4}{a_3}}Y\Big)\operatorname{erfc}\Big(\frac{Y}{2\sqrt{\tau}}+\sqrt{\tau\Big(M+\frac{1}{\chi}-\frac{a_4}{a_3}\Big)}\Big) \\
& +\exp\Big(-\sqrt{M+\frac{1}{\chi}-\frac{a_4}{a_3}}Y\Big)\operatorname{erfc}\Big(\frac{Y}{2\sqrt{\tau}}-\sqrt{\tau\Big(M+\frac{1}{\chi}-\frac{a_4}{a_3}\Big)}\Big)\Bigg] \\
+\frac{a_2}{4a_3\Big(\frac{a_4}{a_3}+I\Omega\Big)}\exp\Big(I\Omega\tau\Big)\Bigg[& \exp\Big(\sqrt{M+\frac{1}{\chi}+I\Omega}\,Y\Big)\operatorname{erfc}\Big(\frac{Y}{2\sqrt{\tau}}+\sqrt{\tau(M+\frac{1}{\chi}+I\Omega)}\Big) \\
& +\exp\Big(-\sqrt{M+\frac{1}{\chi}+I\Omega}\,Y\Big)\operatorname{erfc}\Big(\frac{Y}{2\sqrt{\tau}}-\sqrt{\tau(M+\frac{1}{\chi}+I\Omega)}\Big)\Bigg] \\
+\frac{a_2}{4a_3\Big(\frac{a_4}{a_3}-I\Omega\Big)}\exp\Big(-I\Omega\tau\Big)\Bigg[& \exp\Big(\sqrt{M+\frac{1}{\chi}-I\Omega}\,Y\Big)\operatorname{erfc}\Big(\frac{Y}{2\sqrt{\tau}}+\sqrt{\tau(M+\frac{1}{\chi}-I\Omega)}\Big)
\end{aligned}
$$

$$
\begin{aligned}
&+\exp\Big(-\sqrt{M+\frac{1}{\chi}-I\Omega}\,Y\Big)\operatorname{erfc}\Big(\frac{Y}{2\sqrt{\tau}}-\sqrt{\tau(M+\frac{1}{\chi}-I\Omega)}\Big)\Big]\\
&-\frac{a_2a_4}{2a_3^2\Big(\frac{a_4^2}{a_3^2}+\Omega^2\Big)}\exp\Big(-\frac{a_4}{a_3}\tau\Big)\Big[\exp\Big(\sqrt{M+\frac{1}{\chi}-\frac{a_4}{a_3}}\,Y\Big)\operatorname{erfc}\Big(\frac{Y}{2\sqrt{\tau}}+\sqrt{\tau\Big(M+\frac{1}{\chi}-\frac{a_4}{a_3}\Big)}\Big)\\
&+\exp\Big(-\sqrt{M+\frac{1}{\chi}-\frac{a_4}{a_3}}\,Y\Big)\operatorname{erfc}\Big(\frac{Y}{2\sqrt{\tau}}-\sqrt{\tau\Big(M+\frac{1}{\chi}-\frac{a_4}{a_3}\Big)}\Big)\Big]\\
&-\frac{a_1}{2a_4}\Big[\exp\Big(2\sqrt{PrR}\,Y\Big)\operatorname{erfc}\Big(\frac{Y}{2}\sqrt{\frac{Pr}{\tau}}+2\sqrt{R\,\tau}\Big)\\
&+\exp\Big(-2\sqrt{PrR}\,Y\Big)\operatorname{erfc}\Big(\frac{Y}{2}\sqrt{\frac{Pr}{\tau}}-2\sqrt{R\,\tau}\Big)\Big]\\
&+\frac{a_1}{2a_4}\exp\Big(-\frac{a_4}{a_3}\tau\Big)\Big[\exp\Big(\sqrt{Pr\Big(4R-\frac{a_4}{a_3}\Big)}\,Y\Big)\operatorname{erfc}\Big(\frac{Y}{2}\sqrt{\frac{Pr}{\tau}}+\sqrt{\tau\Big(4R-\frac{a_4}{a_3}\Big)}\Big)\\
&+\exp\Big(-\sqrt{Pr\Big(4R-\frac{a_4}{a_3}\Big)}\,Y\Big)\operatorname{erfc}\Big(\frac{Y}{2}\sqrt{\frac{Pr}{\tau}}-\sqrt{\tau\Big(4R-\frac{a_4}{a_3}\Big)}\Big)\Big]\\
&-\frac{a_2}{4a_3\Big(\frac{a_4}{a_3}+I\Omega\Big)}\exp\Big(I\Omega\tau\Big)\Big[\exp\Big(\sqrt{4R+I\Omega}\,Y\Big)\operatorname{erfc}\Big(\frac{Y}{2\sqrt{\tau}}+\sqrt{\tau(4R+I\Omega)}\Big)\\
&+\exp\Big(-\sqrt{4R+I\Omega}\,Y\Big)\operatorname{erfc}\Big(\frac{Y}{2\sqrt{\tau}}-\sqrt{\tau(4R+I\Omega)}\Big)\Big]\\
&-\frac{a_2}{4a_3\Big(\frac{a_4}{a_3}-I\Omega\Big)}\exp\Big(-I\Omega\tau\Big)\Big[\exp\Big(\sqrt{4R-I\Omega}\,Y\Big)\operatorname{erfc}\Big(\frac{Y}{2\sqrt{\tau}}+\sqrt{\tau(4R-I\Omega)}\Big)\\
&+\exp\Big(-\sqrt{4R-I\Omega}\,Y\Big)\operatorname{erfc}\Big(\frac{Y}{2\sqrt{\tau}}-\sqrt{\tau(4R-I\Omega)}\Big)\Big]\\
&+\frac{a_2a_4}{2a_3^2\Big(\frac{a_4^2}{a_3^2}+\Omega^2\Big)}\exp\Big(-\frac{a_4}{a_3}\tau\Big)\Big[\exp\Big(\sqrt{4R-\frac{a_4}{a_3}}\,Y\Big)\operatorname{erfc}\Big(\frac{Y}{2\sqrt{\tau}}+\sqrt{\tau\Big(4R-\frac{a_4}{a_3}\Big)}\Big)\\
&+\exp\Big(-\sqrt{4R-\frac{a_4}{a_3}}\,Y\Big)\operatorname{erfc}\Big(\frac{Y}{2\sqrt{\tau}}-\sqrt{\tau\Big(4R-\frac{a_4}{a_3}\Big)}\Big)\Big], \qquad (8a)
\end{aligned}
$$

$$\Theta(Y,\tau) = \frac{1}{2}\Big(\Theta_w - 1\Big)\Bigg[\exp\Big(2\sqrt{PrR}Y\Big)\,\mathrm{erfc}\Big(\frac{1}{2}\sqrt{\frac{Pr}{\tau}}Y + 2\sqrt{R\tau}\Big) + \exp\Big(-2\sqrt{PrR}Y\Big)\,\mathrm{erfc}\Big(\frac{1}{2}\sqrt{\frac{Pr}{\tau}}Y - 2\sqrt{R\tau}\Big)\Bigg]$$
$$+\frac{1}{4}\xi\Big(\Theta_w - 1\Big)\exp(I\Omega\tau)\Bigg[\exp\Big(\sqrt{Pr(4R+I\Omega)}Y\Big)\,\mathrm{erfc}\Big(\frac{1}{2}\sqrt{\frac{Pr}{\tau}}Y + \sqrt{\tau(4R+I\Omega)}\Big) + \exp\Big(-\sqrt{Pr(4R+I\Omega)}Y\Big)\,\mathrm{erfc}\Big(\frac{1}{2}\sqrt{\frac{Pr}{\tau}}Y - \sqrt{\tau(4R+I\Omega)}\Big)\Bigg]$$
$$+\frac{1}{4}\xi\Big(\Theta_w - 1\Big)\exp(-I\Omega\tau)\Bigg[\exp\Big(\sqrt{Pr(4R-I\Omega)}Y\Big)\,\mathrm{erfc}\Big(\frac{1}{2}\sqrt{\frac{Pr}{\tau}}Y + \sqrt{\tau(4R-I\Omega)}\Big) + \exp\Big(-\sqrt{Pr(4R-I\Omega)}Y\Big)\,\mathrm{erfc}\Big(\frac{1}{2}\sqrt{\frac{Pr}{\tau}}Y - \sqrt{\tau(4R-I\Omega)}\Big)\Bigg] + 1, \quad (8b)$$

where

$$a_1 = Gr(\Theta_w - 1), \quad a_2 = Gr\,\xi(\Theta_w - 1), \quad a_3 = Pr - 1, \quad a_4 = 4Pr\,R - M - \frac{1}{\chi}, \quad I = \sqrt{-1},$$

and $\mathrm{erfc}\{\cdot\}$ being the complementary error function.

4 Discussion of Results

Equations (8a) and (8b) make it possible to investigate quantitatively the manifestation of the effects of the various parameters entering the problem, and these are M, magnetic parameter; Gr, Grashof number or free convection parameter; χ, porosity parameter; Pr, Prandtl number; Ω, frequency of oscillation, and R, radiation parameter.

For the purpose of physical insights into the problem, the value of ξ is chosen as 1.0, the magnetic field parameter M chosen as $2.0, 5.0, 10.0, 100.0$ and the wall temperature Θ_w as 2.0. The Prandtl number, Pr is set equal to a fixed value of 0.71 throughout the investigations, which physically corresponds to an astrophysical body (air) at $20^o\,C$. Air is chosen because it is weakly electrically conducting under certain circumstances. For the free convection parameter, the value of $Gr = 1.0$ is considered. Typical values of the radiation parameter, R; time, τ; porosity parameter, χ and frequency parameter, Ω used are indicated on the graphs. The maximum value of Y was chosen as 3 after some preliminary investigations so that, the last two boundary conditions (7c) are satisfied (i. e. $U \to 0\,, \Theta \to 1$ as $Y \to \infty$). The appearance of $I = \sqrt{-1}$ in

the solutions (8a) and (8b) is indicative that the solutions are complex. Only the real parts of these solutions are herein graphed for discussions.

Figure 2 is due to the velocity solution for various flow parameters. It is generally observed from Figure 2a, b, c, d that the velocity is both zero at the plate and the edge of the boundary layer. Clearly, the flow satisfactorily obey the initial and boundary conditions. The velocity increases steadily, reaches a maximum and gradually decreases to catch up with the initial state in the boundary layer. In general, the nature of the flow is of parabolic type. We note from Figure 2 that although the boundary layer thickness is $\delta_U \approx 3$, the maximum velocity occurs at $Y \approx 0.5$. This implies that high velocity gradients are observed only near the wall. In Figure 2a, b, c the maximum velocity decreases with increasing radiation, time, magnetic strength. It is noteworthy that the maximum velocity becomes increasingly pronounced as these parameters decreases, indicating that the flow responds more and more sensitively to these parameters within a narrow interval. On the other hand, in Figure 2d the maximum velocity increases with increasing porosity parameter, indicating that the flow responds more sensitively to χ within a wide interval.

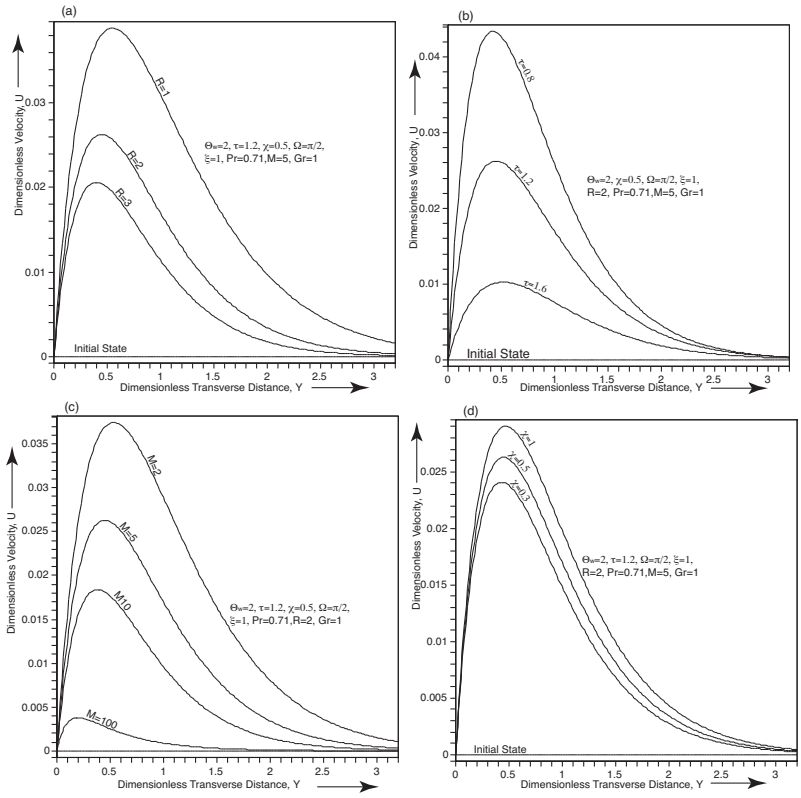

Figure 2: Velocity profiles for variations in the parameters: (a) Radiation, R; (b) Time, τ; (c) Magnetic, M; (d) Porosity, χ.

In particular, Figure 2c depict the influence of the magnetic parameter on the velocity. It is observed that increase in the magnetic parameter reduces the magnitude of the velocity. For sufficiently high M the velocity in the entire flow is virtually constant, and thin boundary layers exist only near the wall. For example, for $M = 100$ the velocity becomes constant half the entire cross section, and only near the wall is the so-called Magnetic layer with high velocity gradient observed. Here the maximum velocity occurs at $Y \approx 0.0039$. The application of the transverse magnetic field plays the role of a resistive type force (Lorentz force) similar to drag force (that acts in the opposite direction of the fluid motion), which tends to resist the flow thereby reducing its velocity. On the other hand, Figure 2d which corresponds to the transient velocity due to increasing χ, physically indicates that the presence of a porous medium increases the resistance to flow and hence when $\chi = \infty$, the effect of porosity vanishes, which implies that the velocity would become greater in the flow field.

Figure 3a, b and c demonstrates the temperature profiles for different values of radiation parameter, time and phase variation, respectively. The magnitude of temperature is maximum at the plate and then decays to zero asymptotically. It is observed from the Figure 3a that an increase in radiation parameter reduces the thermal boundary layer thickness. In Figure 3b it is evident that an increase in time makes the temperature to fall and gives reduction in the thermal boundary layer thickness. Also, it is depicted in Figure 3c that increasing phase angle makes the temperature distribution to fall.

Figure 4a and b, respectively, depicts the periodic temperature distribution with variations of Ω at the surface $Y = 0$ and at a distance $Y = 1$ from the heated surface. It is observed that at the surface $Y = 0$, the temperature reached a maximum value of 3 and gradually reduces to catch up with the initial temperature, whereas at the distance $Y = 1$ from the heated surface, the temperature increases steadily from the initial temperature, attains a maximum and gradually reduces to the initial temperature. The results showed that for $\Omega = \pi/6$, the temperature distribution used minimal times $\tau = 2$ and $\tau = 2.2$ to get to the initial temperature, while for $\Omega = \pi/2$, the temperature distribution used maximal times $\tau = 5.8$ and 5.85 to get to the initial temperature, respectively for Y=0 and Y=1.

Knowing the velocity field, from the practical point of view, it is important to know the effect of the radiation parameter on the skin-friction. The skin-friction at the surface of the plate can be obtained easily from the following non-dimensional relation

$$\tau_s = \frac{\partial U}{\partial Y} \mid_{Y=0} . \tag{9}$$

Table 1 shows values of the skin-friction for variations of radiation and time. It

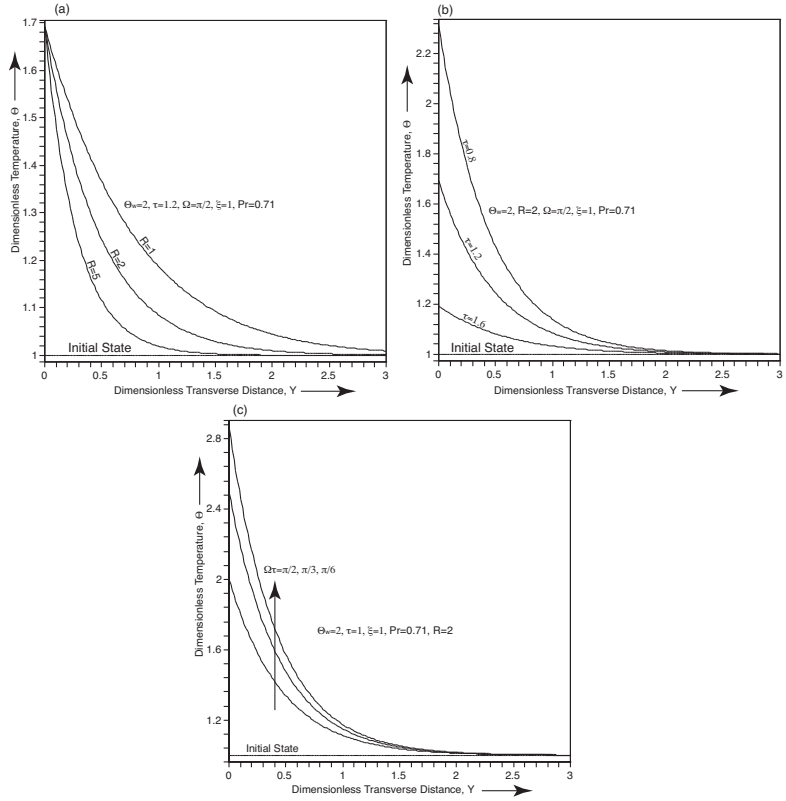

Figure 3: Temperature profiles as a function of Y for variations in the parameters: (a) Radiation, R; (b) Time, τ; (c) Phase Angle, $\Omega\tau$.

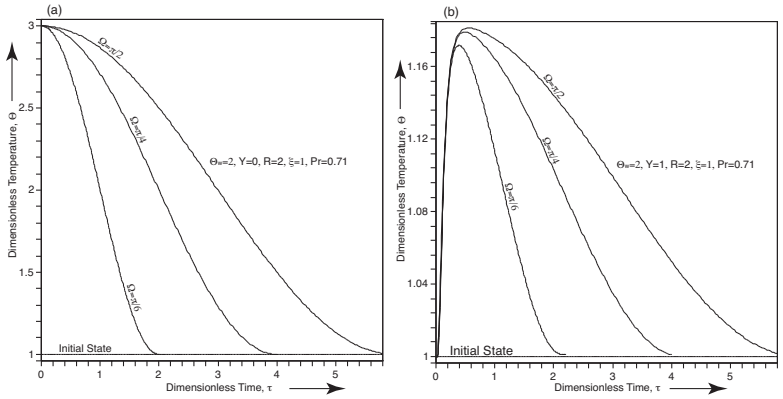

Figure 4: Temperature profiles as a function of τ for variations in the parameters: (a) Frequency, Ω for $Y = 0$; (b) Frequency, Ω for $Y = 1$.

is seen that for both increasing variations of radiation parameter and time, the skin-friction reduces, except for the value of $R = 5.0$ at $\tau = 1.2$, which appears erratic. Generally, the radiation parameter and time shift the fluid gradually away from the plate, thereby reducing the shear on the plate. Of course, this is observed from the Figure 2a, b with time playing a more dominant role than the radiation parameter.

Table 1: Skin friction for variations of Radiation and time: $\Theta_w = 2$, $\Omega = \pi/2$, $\xi = 1$, $\chi = 0.5$, $Pr = 0.71$, $M = 5$, $Gr = 1$.

R	$\tau = 0.8$ Skin Friction	$\tau = 1.2$ Skin Friction	$\tau = 1.6$ Skin Friction
0.0	0.448120	0.303468	0.150877
0.5	0.372543	0.226238	0.088116
1.0	0.328549	0.191651	0.068358
1.5	0.299510	0.171517	0.058640
2.0	0.278496	0.157807	0.052587
2.5	0.262282	0.147577	0.048315
3.0	0.249201	0.139495	0.045076
3.5	0.238305	0.132904	0.040028
4.0	0.228900	0.101047	−0.125862
4.5	0.222186	−0.038309	−0.122198
5.0	0.157914	2999.962321	−0.118900

Knowing the temperature distribution, we can calculate the rate of heat flux, q_w , between the fluid and the wall of the plate. This is calculated from

$$q_w = \frac{\partial \Theta}{\partial Y} \mid_{Y=0}, \tag{10}$$

by virtue of equations (5). Table 2 accounts for effects of variations of radiation parameter with respect to time on the heat flux. It is observed that for a given time, the heat flux decreases with increasing radiation, and for a given radiation, the heat flux increases with increasing time. The negative values of the wall temperature gradient, are indicative of the physical fact that the heat flows from the plate surface to the ambient fluid.

5 Concluding remarks

The problem of the effect of thermal radiation on transient MHD free convection flow over a vertical surface embedded in a porous medium with periodic temperature has been examined. Analytical solutions of the flow variables are presented. Some physical parameters were identified entering the problem.

Table 2: Heat flux for variations of Radiation and time: $\Theta_w = 2$, $\Omega = \pi/2$, $\xi = 1$, $Pr = 0.71$.

R	$\tau = 0.8$ Heat Flux	$\tau = 1.2$ Heat Flux	$\tau = 1.6$ Heat Flux
0.0	−0.133407	0.464618	0.641843
0.5	−1.201559	−0.391211	0.090880
1.0	−1.911244	−0.846424	−0.105841
1.5	−2.453020	−1.166046	−0.222694
2.0	−2.901896	−1.421827	−0.309106
2.5	−3.292097	−1.640235	−0.379658
3.0	−3.641514	−1.833686	−0.440377
3.5	−3.960615	−2.009037	−0.494330
4.0	−4.256080	−2.170519	−0.543295
4.5	−4.532461	−2.320945	−0.588402
5.0	−4.793021	−2.462298	−0.630419

It is generally observed that the flow variables are significantly influenced by these parameters.

The primary findings are summarized as follows:

- The velocity increases and attains its maximum value in the vicinity of the plate and then fades away to zero as $Y \to \infty$.
- The temperature of the fluid decreases with increasing radiation. While increasing radiation signifies reduction in the maximum velocity, for the temperature it decreases the thermal boundary layer thickness, physically implying higher heat transfer to the plate.
- It is observed that increasing magnetic parameter reduces the magnitude of the velocity. For sufficiently high M the velocity in the entire flow is virtually constant, and only near the wall is the so-called Magnetic layer with high velocity gradient or thin boundary layer observed.
- The velocity increases with increasing porosity parameter. Physically, this implies that the presence of a porous medium increases the resistance to flow, and greater velocity is experienced in the flow field when the porosity parameter vanishes.
- The maximum velocity decreases with an increase in phase angle.
- The temperature decreases with an increase in phase angle.
- Increase in radiation parameter decreases the skin-friction and heat flux.

It is hoped that the present investigation may serve as toolkits for the verification of the efficiency and accuracy of numerical implementations. It is noted here that the efficient computation of thermal radiation effect is essential for the design and analysis of industrial thermal systems, such as furnaces, boilers, burners, nuclear power plants, combustion products (such as H_2O and CO_2) and gas turbines. The results of the problem are also of great interest in geophysics in the study of interaction of the geomagnetic field with the fluid in the geothermal region.

References

[1] J. F. N. Abowei and F. D. Sikoki, *Water Pollution Management and Control*, (Doubletrust Publications Company, Port Harcourt, Nigeria, 2005).

[2] B. M. Abramowitz and I. A. Stegun, *Handbook of Mathematical Functions*, (Dover, New York, 1964).

[3] A. R. Bestman and S. N. Adjepong, Unsteady hydromagnetic free-convection flow with radiative heat transfer in a rotating fluid. *Space Sci.*, **143** (1988), 73 - 80.

[4] H. Branover, *Magnetohydrodyamic Flow in Ducts*, (John Wiley and Sons, Ltd., 1978).

[5] R. C. Chaudhary and A. Jain, Magnetohydrodynamic Transient Convection Flow past a Vertical Surface Embedded in a Porous Medium with Oscillating Temperature, *Turkish J. Eng. Env. Sci.*, **32** (2008), 13 - 22.

[6] P. Cheng, *Proc. NATO Advanced Study in Natural Convection*, (Izmir, Turkey, 1985).

[7] P. Cheng. and W. J. Minkowycz, Freeconvection about a vertical flat plate embedded in a porous medium with application to heat transfer from a dike, *J. Geophys. Res.*, **82**, 14 (1977), 2040 - 2044.

[8] T. J. Chung, *Computational Fluid Dynamics*, (Cambridge University Press, UK., 2002).

[9] A. C. L. Cogley, W. G. Vincenti and E. S. Gilles, Differential approximation for radiative heat transfer in a nonlinear equations-grey gas near equilibrium. *Am. Inst. Aeronaut. Astronaut. J.*, **6** (1968), 551 - 553.

[10] J. C. T. Eijkel, A. Van den Berg and A. Manz, Cyclic electrophoretic and chromatographic separation methods. *Electrophoresis*, **25** (2004), 243 - 252.

[11] S. Fan and J. R. Barber, Solution of periodic heating problems by transfer matrix method, *Int. J. Heat Mass Transfer*, **45** (2002), 1155 - 1158.

[12] F. K. Gbaorun, B. Ikyo, B. Iyorzor and R. Okanigbun, A heat model for temperature distribution in a laptop computer, *J. of NAMP*, **12** (2008), 201- 206.

[13] P. S. Ghoshdastidar, *Heat Transfer*, (Oxford University Press, UK, 2004).

[14] J. R. Howard and A. E. Sutton, An analogue study of heat transfer through periodic contacting surfaces, *Int. J. Heat Mass Transfer*, **13** (1970), 173 - 183.

[15] C. Israel-Cookey, P. Mebine and A. Ogulu, MHD free-convection and mass transfer flow on a porous medium in a rotating fluid due to radiative heat transfer. *AMSE Modell. Mass. Control B*, **71**, 2 (2002), 1 - 7.

[16] R. Korycki, Sensitivity analysis and shape optimization for transient heat conduction with radiation, *Int. J. Heat Mass Transfer*, **49** (2006), 2033 - 2043.

[17] A. V. Lemoff and A. P. Lee, An AC magnetohydrodynamic micropump. *Sensors and Actuators B*, **63** (2000), 178 - 185.

[18] P. Mebine, Thermosolutal MHD flow with radiative heat transfer past an oscillating plate, Advances in Theoretical and Applied Mathematics. *Advances in Theoretical and Applied Mathematics*, **2**, 3 (2007), 217 - 231.

[19] P. Mebine, Radiation Effects on MHD Couette Flow with Heat Transfer between Two Parallel Plates, *Global Journal of Pure and Applied Mathematics*, **3**, 2 (2007), 1 - 12.

[20] S. Middleman, *An Introduction to Mass and Heat Transfer*, (John Wiley & Sons, Inc., 1998).

[21] D. A. Nield and A. Bejan, *Convection in Porous Media*, (Springer, Berlin, 1992).

[22] J. Peterson, N. Tuttle, H. Cooper and C. Baukal, Minimize facility flaring, *Hydrocarbon Processing*, (2007), 111 - 115.

[23] S. Qian and H. H. Bau, Magneto-hydrodynamics based microfluidics, *Mechanics Research Communications*, **36** (2009), 10 - 21.

[24] H. Rubin and J. Atkinson, *Environmental Fluid Mechanics*, (Marcel Dekker, Inc, New York, 2001).

[25] J. West, B. Karamata, B. Lillis, J. P. Gleeson, J. Alderman, J. K. Collins, W. Lane, A. Mathewson and H. Berney, Application of magnetohydrodynamic actuation to continuous flow chemistry. *Lab on a Chip* **2** (2002), 224 - 230.

[26] J. West, J. P. Gleeson, J. Alderman, J. K. Collins and H. Berney, Structuring laminar flows using annular magnetohydrodynamic actuation. *Sensors and Actuators B*, **96** (2003), 190 - 199.

[27] J. Zhong, M. Yi and H. H. Bau, Magneto hydrodynamic (MHD) pump fabricated with ceramic tapes. *Sensors and Actuators A*, **96** (2002), 59 - 66.

Received: February, 2011